COBEM2015

ABCM Associação Brasileira de Engenharia e Ciências Mecânicas

23rd ABCM International Congress of Mechanical Engineering
December 6-11, 2015, Rio de Janeiro, RJ, Brazil

REACTIVE DYNAMICS CAUSED BY IMPULSIVE FORCES

Gustavo Simão Rodrigues
Hans Ingo Weber
Pontifícia Universidade Católica do Rio de Janeiro. Rua Marquês de São Vicente, 225 - Gávea, Rio de Janeiro - RJ, 22451-900
gustavosimao@uol.com.br
hans@puc-rio.br

Abstract. *The purpose of this study is to analyze the behavior of a system under the action of an impulsive force by experimental observations obtained with a specially built device. The action of impulsive forces is quite dependent of the particular application. Sometimes it matters to have this force at a maximum, like when you use it to excite, or to have a perfect profile of the impulse to excite a maximum amount of resonances of a system and sometimes you want to avoid that internal impulsive efforts reflect on the overall behavior of the dynamics of a specific system. In addition, we intend to compare the results obtained in the experiment with current mathematical collision models, or force laws, inspired by models used in several studies on the Newton's cradle, where the impact velocity before the collision is evaluated, as well as the velocities of the bodies after collision. Thereby we intend to estimate the stiffness of the components and their damping constant by using mathematical models simulated in MATLAB to verify experimentally the results. Finally, the most important result is to identify how to absorb the impulse before it disturbs the desired overall behavior of the system that contains the disturbance.*

Keywords: *impulsive force, body collision, Newton's Cradle experiment*

1. INTRODUCTION

The research of contact mechanics started over a century ago, in 1882, with Hertz and since then many other works were developed in this field. One of the objectives in this area is to understand granular flows. Cundall and Strack (1979) were the pioneers using discrete particle approach in the description of granular materials. Hertzsch (1995) studied collisions of viscoelastic particles. Stevens and Hrenya (2005) compares soft-sphere models to measurements of collision properties during normal impacts. Donahue *et. al*. (2010) consider three-body collisions between wetted particles. Most of the papers in this field treat identical spheres collisions and they are interested in predict post-collisional velocity and estimate duration of contact between the bodies.

The force acting between two bodies during collision is characterized by a high intensity and an infinitesimal duration. This force is called impulsive force and appears in many situations as car crashes, kicking a ball, a putter throwing a golf ball, a recoil system of a gun or hammering a nail.

It was observed that all collected theory of contact during collision take into account identical spheres, except for the work Lovett *et. al.* (1988) considering spheres of different sizes.

Thinking about a real situation of contact between different bodies, we intend to find out formulations to model systems under action of impulsive forces as similar as possible of reality. The system analyzed in the present work is shown in Fig. 1.

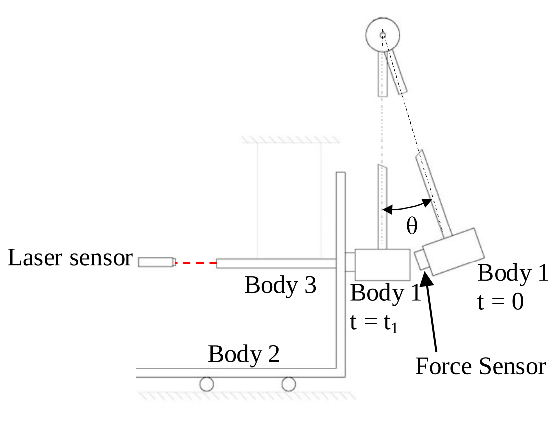

Figure 1. Physical model of the system to be analyzed

The experimental apparatus used in this work is a first idealization to verify the viability of the research in this area before a more detailed construction. All results refer to this preliminary part of the research.

2. EXPERIMENTAL METHOD

The experiment was assembled in order to become the most similar to the idealized system shown in Fig. 1. Thus, body 1 is composed by a mass connected to a rod on one end. In this same end, we fixed a force sensor to measure the impact force. On the other end, the rod is fixed by a bearing and can rotate almost free from friction. Body 2 was attached to a rail to minimize friction, so it will be considered negligible. Body 3 is suspended by nylon wires in a way that it can be considered free from external interaction, i.e., the only force acting on body 3 is the transmitted force by body 2.

The experiment uses a Micro-epsilon laser sensor, model LD1607-20, with range of 55 to 75 mm used to compute the displacement along time, i.e., to calculate velocity.

To compute the impact force, we used a PCB force sensor, model 208C03 SN 27576, with 2.224 mV/N sensibility and 2225 N range.

The information is captured by a Tektronix oscilloscope, model TDS 2024B, recorded directly on a flash removable drive via USB port and the data is processed by MATLAB software to obtain the desirable outcomes.

2.1 Experimental assembly

Body 1 is a kind of hammer composed by an axle of brass, a rod made of stainless steel and a steel head connected at the end of the rod. This sub-assembly is shown in Fig. 3.

Body 2 is steel "L" shape with base 240 mm, height 225 mm, depth 215 mm and thickness 10 mm. "L" shape base is made of aluminum and "L" shape vertical wall is made of steel, both attached by screws. Total "L" shape mass, i.e., body 2 mass is 4753 g.

Body 3 is a sheet of steel with 131 x 90 x 10 mm. The properties of Body 3 are Young's modulus E=2.03x10^{11} N/m^2, Poisson's ratio ν =0.28, yield strength Y=2.03x10^9 N/m^2, mass m=880 g.

Figure 3 shows the experiment assembly used in this paper.

Figure 2. Experimental assembly

2.2 Calculation of impact velocity

As said above, body 1 is a kind of hammer and was modeled in 3D CAD software, illustrated in Fig. 3. Utilizing a software functionality it is possible to determine exactly the center of mass besides the momentum of inertia, data needed to calculate the impact velocity for each initial position. The impact velocity is considered when Body 1 is on the bottom of the arc of displacement, so the other bodies are positioned to guarantee this configuration.

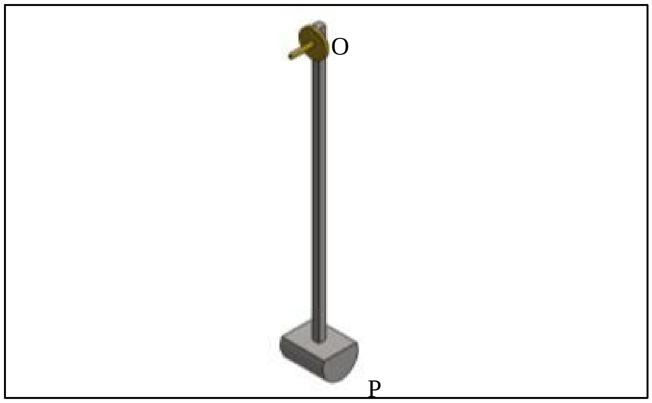

Figure 3. Body 1 represented by a hammer 3D modeled.

Rigid body mechanics (Rao, 2009) provides body 1 dynamics formulation.

$$J_0\ddot{\theta} + Wd\,\theta = 0 \tag{1}$$

Where J_0 is the momentum of inertia taken at point of rotation O, W is the weight of the hammer and d is the distance between the point of rotation O and center of mass. The values obtained in 3D CAD software for J_0 is 1238.90 kg.cm^2, d is 32.5 cm and mass is 1008 g, i.e., W is 9.888 N using gravity acceleration 9.81 m/s^2.

Momentum of inertia value is validated measuring the hammer oscillation period (T) and Eq. (2) and Eq. (3) allow we calculate the momentum of inertia, using the measured value:

$$\omega^2 = \frac{Wd}{J_o} \tag{2}$$

$$T = \frac{2\pi}{\omega} \tag{3}$$

The mean of 20 measured values of period was 1.22 seconds. Using the parameters W and d given above, we found a momentum of inertia value of 1214.6 kg.cm^2, which yield less than 2% of difference between momentum of inertia calculated on 3D CAD software and calculated by measuring the oscillation period. So we accept the mean between both momentum of inertia, i.e., J_0 is 1226.75 kg.cm^2 for all calculation.

Remembering that Eq. (1) works for small values of θ, it is possible calculate the velocity of point P at the instant of impact by solving the initial value problem where $\theta(0) = \theta_0$ and $\dot{\theta}(0) = 0$. Figure 4.a) shows the Hammer rest position, which is also considered the impact position and Fig. 4.b) shows the hammer at the marking of position $\theta_0 = 10^o$, for example.

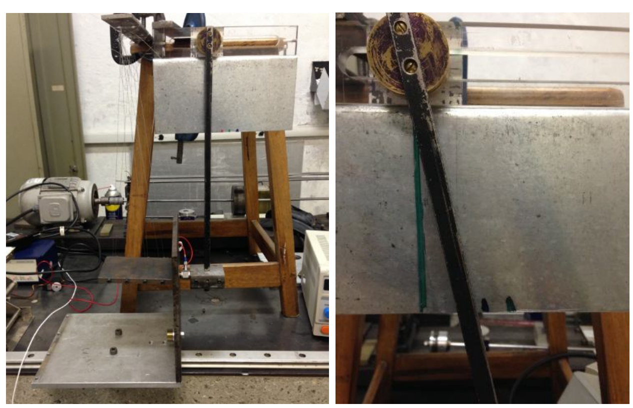

Figure 4. a) Hammer rest position. b) Hammer initial position at 10°.

Using again the 3D CAD software, we found point P is 37.7 cm from point of rotation O. For some initial values θ_0, we have the impact velocities summarized in Table 1.

Table 1. Calculated body 1 velocities V_1 for initial positions θ_0

θ_0 (degrees)	ω_1 (rad/s)	V_1 (m/s)
10	0.893	0.336
15	1.340	0.505
20	1.787	0.673

2.3 Measured impact force

To obtain the impact force at positions determined above, we used PCB force sensor especificated in item 2. For example, the recorded profile of impact force is shown in Fig. 5 is the oscilloscope display.

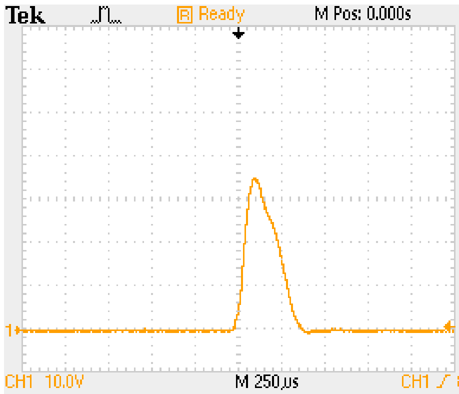

Figure 5. Oscilloscope display

3. DEVELOPED THEORY

3.1 Collisional models of three body interaction

As known, Newton's Cradle is composed of identical spheres. Let's take for example Newton's Cradle with three spheres. The first one is released at a height, h, and impacts the second sphere, which is in touch with the third sphere and both second and third spheres are initially at rest at the bottom of the pendulum arc. It is considered that the second sphere receives a normal impact of the first one. First sphere impact velocity is $v_1 = \sqrt{2gh}$ due to the released height. If there was a perfect conservation of momentum and energy, we would expect a total transfer of momentum from sphere one to sphere three and after collision, both spheres one and two would remain in rest and sphere three would leave with velocity $v_3 = \sqrt{2gh}$.

However, we know that friction and energy losses in real world exist. That's the reason why we look for a better way to represent normal collision, namely soft sphere collision model.

As said above, Hertz was the first to study and develop a mathematical approach to contact forces during collisions. Hertz model takes into account perfectly elastic particles. He considered that during contact, particle deformation is defined by sphere's overlap. The overlap, δ, is defined as

$$\delta = \max(0, x_i - x_j) \tag{4}$$

Where x_i and x_j are the positions of bodies i and j, respectively, at the exact moment of contact. So, the difference $x_i - x_j$ is considered the amount of overlap of body i over body j.

This deformation generates a repulsive force between the particles. The repulsive force in Hertz model, F_n, is

$$F_n = k_n \delta^{1.5} \tag{5}$$

Where k_n is the stiffness between spheres in collision. Based on the spheres radius, Young's modulus and Poisson's ratios it is possible to estimate the stiffness k_n. However, in this work we don't have any spheres so we will define the stiffness as explained in section 4.

The other model widely used is linear-spring and dashpot (LSD), which also takes into account the rate of deformation, as shown in Eq. (6). (Donahue, *et. al*., 2008).

$$F_n = k_n\delta + \beta_n\gamma_{n,crit}(\frac{d\delta}{dt}) \tag{6}$$

Here we define $\beta_n\gamma_{n,crit}$ as a damping factor namely α_n, since β_n and $\gamma_{n,crit}$ are calculated due to spheres features and the bodies used in this paper aren't spheres. Hence, Eq. (6) becomes in this paper the LSD model:

$$F_n = k_n\delta + \alpha_n(\frac{d\delta}{dt}) \tag{7}$$

Kuwabara and Kono (1987) proposed a model that is a variation of Hertz model and LSD model, more specifically, a combination of both Hertz and LSD models. Equation (8) shows their model, called KK model:

$$F_n = k_n\delta^{1.5} + \gamma_n\delta^{0.5}(\frac{d\delta}{dt}) \tag{8}$$

4. RESULTS

To compare the measured velocity of body 3 and the calculated one, the impulsive force measured will be transformed into initial velocity of body 2 using the principle of linear impulse and momentum:

$$L = \int_{t_1}^{t_2} F\ dt = mv_2 - mv_1 \tag{9}$$

Remember that its initial velocity is zero ($v_1 = 0$) and the integral in this equation is the area under the curve presented in Fig. 5.

Hertz model shown in Eq. (5) will be used to calculate velocity of body 3. The value of stiffness used will be the same used in Donahue, *et. al.* (2008) for stainless steel spheres, namely $k_n = 1.17\text{x}10^{10}\ N/m^{\frac{3}{2}}$. It was noted that varying k_n, the final velocity doesn't change. The modification observed using different k_n is in contact time, decreasing as k_n increases.

Releasing body 1 from an angle of approximately 10°, we obtain the impact force shown in Fig. 5. Note that the initial position doesn't need to be accurate because regardless of the initial position, the input data is the measured impact force. Data obtained experimentally is used to plot in MATLAB Fig. 6. Thus, the value of the peak is 35 V, which converted provides a value of 15.74 kN.

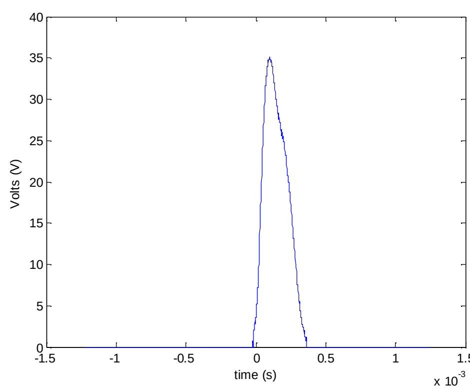

Figure 6. Data plotted in MATLAB

This curve is Volts (V) x time (s) and there isn't a function that describes this behavior once this is an array plot. However, the area under the curve in Fig. 6.b) can be determined numerically because the displacement between each point is equally spaced, namely the sample interval $1\text{x}10^{-6}$ s, information provided by the oscilloscope. Thus, the area under the curve in Fig. 6, i.e., the impulse, is easily calculated summing all terms of Voltage and multiplying by the sample interval, wich results 7.156 mV.s. Using sensor sensibility, 2.224 mV/N, it's possible to convert 7.156 mV.s to 3.18 N.s.

We also calculated the duration period of the impact force in Fig. 6. The value of $3.87 \text{ x } 10^{-4}$ s was found for this measurement.

Using the method described above, we calculated the impulse of the impact force as 3.18 N.s giving an initial velocity of body 2 of 0.669 m/s. This initial velocity is applied in Hertz model as initial condition of Eq. (5), which provides a velocity of 1.216 m/s of body 3. This result is presented in Fig. 7.b). In Fig. 7.a) we can see body 2 has initial velocity imposed of 0.669 m/s and final velocity of 0.547 m/s.

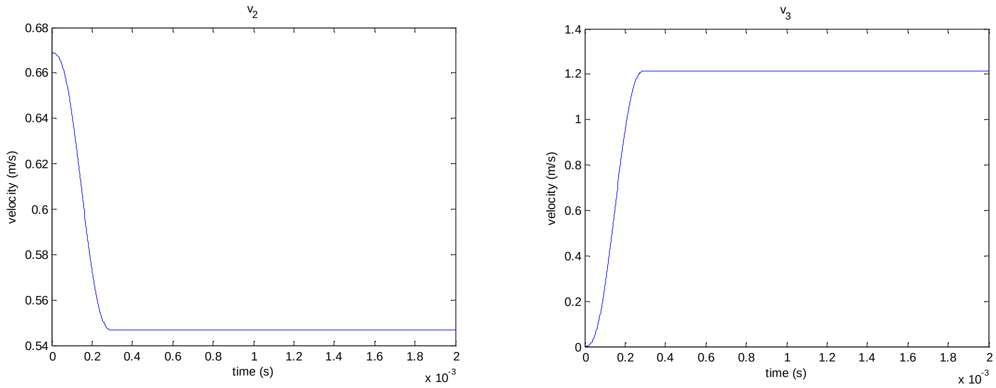

Figure 7. a) Body 2 velocity variation b) Body 3 velocity variation

Figure 8.a) presents displacement of body 3 after the impact force excites the system extracted from oscilloscope. Figure 8.b) is data obtained plotted in MATLAB.

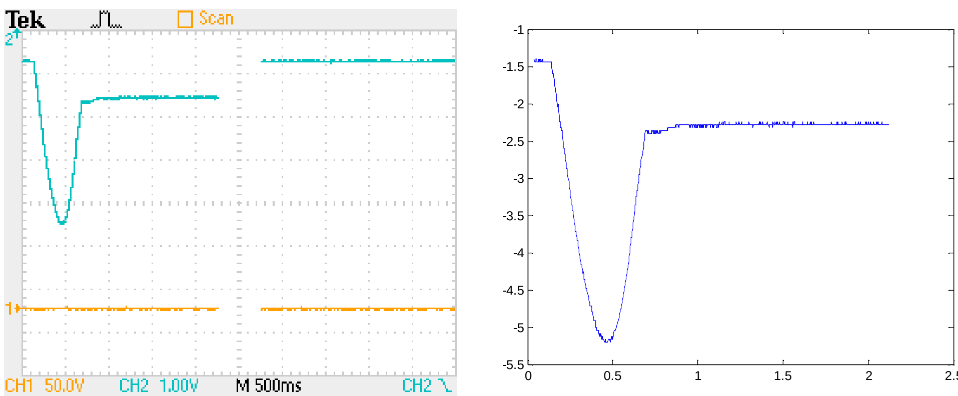

Figure 8. a) oscilloscope display b) data plotted in MATLAB

In Fig. 9.a) is possible observe a curve that approximate linearly data in the part of beginning of displacement. Figure 9.b) is a detailed view of this most important part of the graphic.

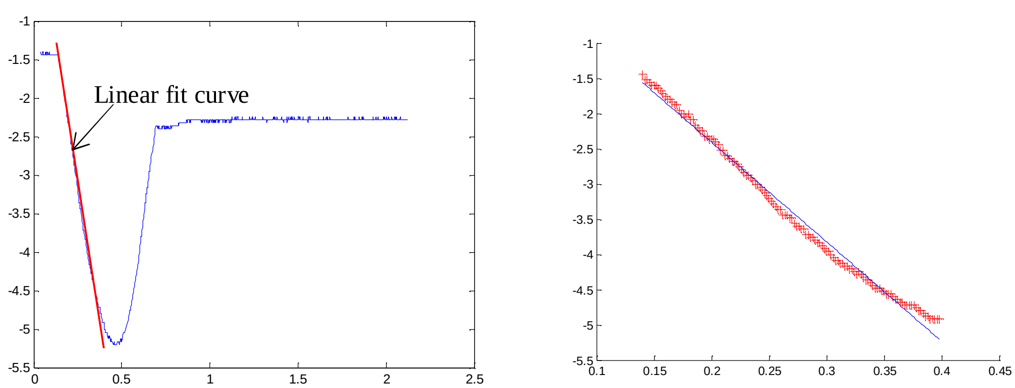

Figure 9. a) Linear fit curve b) linear fit curve detail

Once defined the linear fit curve, the slope of the curve will provide the velocity of body 3. For the initial condition proposed, i.e., hammer initial position of approximately 10°, we obtain a measured velocity of body 3 of 0.967 m/s.

Table 2 concentrate all response for various initial conditions.

Table 2. Response of system for considered initial conditions

θ_0 (degrees)	Impulse (N.s)	Initial velocity of body 2 (m/s)	Calculated velocity of body 3 (m/s)	Measured velocity of body 3 (m/s)
10	3.18	0.669	1.216	0.967
15	4.47	0.941	1.710	1.522
20	6.01	1.265	2.298	1.940

5. CONCLUSIONS

We observe that the measured velocity is not in accordance with the calculated one using Hertz model, indicating that model used is not accurate enough to predict final velocity.

The other models presented in item 3.1 probably will not provide significant improvement because they are all based on Hertzian Contacts.

In this paper, as an incipient study of the mechanical contact phenomenon, precision is not primordial, but a first simplified investigation to define directions of next steps.

In future works we intend apply other contact mechanic models, namely Non-Hertzian contact models. These models are studied since the 70s by Kalker and Van Randen (1972) and may describe more accurately collisions between different bodies.

6. ACKNOWLEDGEMENTS

We thank Coordenação de Aperfeiçoamento de Pessoal de Nível Superior (CAPES) and Pontifícia Universidade Católica of Rio de Janeiro (Brazil).

7. REFERENCES

Cundall, P. A. and Strack, O. D. L., 1979. “A discrete numerical model for granular assemblies”. Geotechnique 29, 47.

Donahue, C. M., Hrenya, C. M., Davis, R., Nakagawa, K., Zelinskaya, A., and Joseph, G., 2010. “Stokes' cradle: normal three-body collisions between wetted particles.” Journal of Fluid Mechanics, 479.

Donahue, C. M., Hrenya, C. M., Zelinskaya, A. P. and K. J. Nakagawa, 2008. “Newton’s cradle undone: Experiments and collision models for the normal collision of three solid spheres”. Phys. Fluids, 20.

Hertz, H., 1882. “On the Contact of Rigid Elastic Solids and on Hardness”. Journal fur die Reine und Angewandte Mathematik 94:156-71.

Hertzsch, J., M., F. Spahn, F., and Brilliantov, N.V., 1995. “On Low-Velocity Collisions of Viscoelastic Particles”. J. Phys. I (Paris), 6:5.

Hibbeler, R. C., 2012 . “Engineering Mechanics: Dynamics”. 13th Edition, Prentice Hall.

Kalker, J.J., and Van Randen, Y. 1972. “A minimum principle for frictionless elastic contact with application to non-Hertzian half-space contact problems”, J. Engng. Math., 6 193-206.

Kuwabara, G. and Kono, K., 1987. “Restitution coefficient in a collision between two spheres,” Jpn. J. Appl. Phys., Part 1 26, 1230.

Lovett, D. R., Moulding, K. M., and Anketell-Jones, S. 1988. “Collisions between elastic bodies: Newton's cradle”. European Journal of Physics 9 (4): 323.

Rao, S. S., 2009. “Mechanical Vibration,” 4th Edition, Prentice Hall.

Stevens, A. B. and Hrenya, C. M., 2005. “Comparison of soft-sphere models to measurements of collision properties during normal impacts,” Powder Technology, Vol. 154, pp. 99 – 109.

8. RESPONSIBILITY NOTICE

The authors are the only responsible for the printed material included in this paper.